参考著作No.8

ASCE | LIBRARY

SEARCH CART LOG IN / REGISTER

JOURNALS BOOKS MAGAZINE AUTHOR SERVICES USER SERVICES

Journal of Performance of Constructed Facilities / Volume 32 Issue 3 - June 2018

Technical Papers

Downloaded 197 times

DETAILS FIGURES REFERENCES RELATED

Reliability Analysis of River Bridge against Scours and Earthquakes

Kuo-Wei Liao; Yasunori Muto; and Jessica Gitomarsono

FULL TEXT DOWNLOAD TOOLS SHARE

Authors

Kuo-Wei Liao

Associate Professor, Dept. of Bioenvironmental Systems Engineering, National Taiwan Univ., No. 1, Section 4, Roosevelt Rd., Taipei 10617, Taiwan (corresponding author). E-mail: kliao@ntu.edu.tw

参考著作No.8

Reliability Analysis of River Bridge against Scours and Earthquakes

Kuo-Wei Liao[1]; Yasunori Muto[2]; and Jessica Gitomarsono[3]

Abstract: This study proposes a bridge safety evaluation process against seismic and flood hazards. Because uncertainties in the scours, seismic hazard, and structural performance for a given seismic excitation are inevitable and important, reliability analysis is adopted. A scour prediction equation for a bridge with a complicated foundation system is developed and a probabilistic scour curve is constructed to measure the risk of scours using the Monte Carlo simulation. The seismic hazard is measured using the probabilistic seismic-hazard analysis. A series of nonlinear time-history analyses are performed to determine the structural performance under different peak ground acceleration values. Specific software is used to build the finite-element model where the soil is modeled using a bilinear link. A plastic hinge is predefined to simulate the nonlinear behaviors of the pier and caisson of the bridge. The displacement ductility is used to measure the structural performance and to construct the fragility curve for various limit states. The Nanyun Bridge located in central Taiwan is selected as an example to demonstrate the proposed safety evaluation procedure. The results show that the probable scour depth of the Nanyun Bridge is from 3 to 5 m. The failure probability considering the floods and earthquakes is insignificant. A deterministic design value, considering both the hazards, is provided for a given reliability target (e.g., $\beta = 3$) to help engineers in their present design processes. **DOI: 10.1061/(ASCE)CF.1943-5509.0001153.** *© 2018 American Society of Civil Engineers.*

Author keywords: Seismic excitation; Reliability analysis; Multihazards; Scour depth; Displacement ductility.

Downloaded from ascelibrary.org by NTU on 07/11/18. Copyright ASCE. For personal use only; all rights reserved.

Introduction

In earthquake engineering, many efforts are targeted on correlating earthquake intensities and damages of buildings or bridges. Basoz et al. (1999) developed a fragility curve for empirical relationship between ground motion and bridge damage for Northridge earthquake, in which the California Department of Transportation (Caltrans) defined the damage states. Based on the on-site investigation, Hsu and Fu (2004) found several types of bridge damage in the Chi-Chi earthquake such as unseating span failure, abutment failure, joint failure, substructure damage, footing settlement, and so on. Elnashai et al. (2012) analyzed the earthquake effect on the buildings and bridges for the Chile earthquake. They first developed site specific ground motions and then several typical failures observed in the engineered buildings and bridges were investigated. Based on the field investigation, it was found that excessive displacements of the superstructure lead to unseating and collapse of several bridges. The on-site bridge damage reports often implied that earthquake-induced damage is not easily classified. However, displacement related damage is often found on the field and is a suitable choice to measure the bridge performance under earthquake excitations.

In addition to the earthquake hazard, flood hazard is another important risk that should be considered. For example, Padgett et al. (2008) reported that 44 bridges were damaged from Hurricane Katrina. Bridge damage is primarily due to debris impact. According to Andrić and Lu (2016), the potential hazards for a bridge are classified as geological, windstorms, and hydraulic hazards, in which geological hazards include earthquake, tsunami, liquefaction, soil, and landslides; hydraulic hazards include flood, debris, scour, and drift. Based on literature survey, the primary reason for bridge damage in the United States is related to flood-induced damage. According to a report of Construction Research Institute in Taiwan, bridges in Taiwan also have the same trend. Taiwan is a seismically active and flood-prone region. Thus, the goal of this study to investigate the bridge performance under earthquake attacks in the presence of flood-induced scour. To be specific, this study is aimed at evaluating the joint-failure probability of a river bridge subjected to multihazard conditions.

There are thousands of bridges in Taiwan. Many of these bridges were built several decades ago and need to be examined to ensure operational safety. Among the different disasters, floods and earthquakes frequently occur in Taiwan and their influences are significant. Typhoon-induced floods often result in a serious scour problem. This study considers the two hazards simultaneously to ensure the safety of the bridge. Many uncertainties are involved in the considered hazards, and therefore a probabilistic approach is adopted. The reliability of the bridge is calculated considering uncertainties in the scours, seismic hazard, and structural performance under a given seismic excitation.

Many formulae have been proposed to determine the scour depth. Melville and Coleman (2000) and Hydraulic Engineering Circular No. 18 (HEC-18 2012) provide methodologies to consider the nonuniform pier effect. To employ the uniform pier formula, Melville and Coleman (2000) converted the nonuniform pier width to an equivalent uniform pier width to predict the scour depth. However, in HEC-18, the considered foundation was divided into three parts and the scour depth of each part was calculated separately. In earlier times, the nonuniform foundation effect was rarely considered. Thus, scour depth is often calculated using the approach of uniform pier formula in Taiwan. To avoid extra burden

[1]Associate Professor, Dept. of Bioenvironmental Systems Engineering, National Taiwan Univ., No. 1, Section 4, Roosevelt Rd., Taipei 10617, Taiwan (corresponding author). E-mail: kliao@ntu.edu.tw

[2]Professor, Dept. of Civil and Environmental Engineering, Tokushima Univ., Tokushima 770-8501, Japan.

[3]Formerly, Graduate Student, National Taiwan Univ. of Science and Technology, Taipei 10617, Taiwan.

Note. This manuscript was submitted on March 28, 2017; approved on November 2, 2017; published online on March 27, 2018. Discussion period open until August 27, 2018; separate discussions must be submitted for individual papers. This paper is part of the ***Journal of Performance of Constructed Facilities***, © ASCE, ISSN 0887-3828.

in practice, the approach used by Melville and Coleman is employed to develop a scour-prediction formula using collected scour data and an optimization algorithm. Note that this selection does not include an accuracy judgement between Melville and Coleman's approach and HEC-18. Further, a probabilistic scour curve is constructed to measure the risk of scours using the Monte Carlo simulation (MCS).

The seismic hazard is evaluated using probabilistic seismic hazard analysis (PSHA). To obtain the structural performance under different peak ground acceleration (PGA), the nonlinear time-history analysis is performed where seven recorded ground motions published in the Pacific Earthquake Engineering Research (PEER) ground motion database are used. The ground motions are fitted and scaled to the response spectrum at the bridge location using the Taiwan code corresponding to the return periods of 475 and 2,500 years. The mechanical properties of the cover and core concretes are considered. The detailed modeling procedure of the concrete mechanism is provided in the section "Simulation of Nonlinear Behaviors of Pier and Caisson." The simulations of the plastic hinges of the pier and caisson are major factors in this mechanism.

The displacement ductility is used as the parameter in constructing the fragility curve. A finite-element model of the Nanyun Bridge is built to apply the proposed methodology. In the end, a design scour depth, which is a deterministic value, is provided to help engineers in their practice. That is, if the safety of a bridge with design scour depth is ensured by the current practice, such bridge will meet the target reliability for both the hazards. Several values for target reliability have been suggested (Honjo et al. 2002), ranging from 1.75 to 7.5 for different structural member (e.g., beam in shear or wall in compression) and different failure mechanism (e.g., ductile or brittle). Using $\beta = 3$ as the target reliability, which is roughly equal to the threshold value (1.00×10^{-3}) suggested by the ISO (Davis-McDaniel et al. 2013), is often acceptable and therefore is adopted in this study.

Proposed Methodology

Fig. 1 shows the flowchart of the proposed methodology. The joint-failure probability of a bridge is the product of three probabilities (Alipour et al. 2013): the probability of seismic hazard, scour depth, and bridge failure for a given limit state. The seismic hazard developed by the National Center for Research on Earthquake Engineering (NCREE) is adopted in this study (Yeh and Jean 2007). From the experiments, 176 scour depths are obtained to develop a scour-prediction formula using the methodology proposed by Melville and Coleman (2000). Subsequently, a probabilistic scour curve is established. The fragility analysis is a common tool to determine the structural-failure probability under different limit states. To build the fragility curve, several nonlinear time-history analyses are conducted. The fragility curve is a conditional probability where the condition refers to a given scour depth. Thus, a predefined scour depth is given for the bridge model in the time-history analysis. Because the modeling of a bridge plays an important role in evaluating the structural performance, the nonlinear behaviors of the pier, caisson, and soil are carefully simulated. The details of the proposed methodology are provided in the following sections.

Building the Probabilistic Scour Curve

Melville and Coleman (2000) proposed a formula to predict the scour depth of a complicated foundation. The calculation method is expressed in Eq. (1)

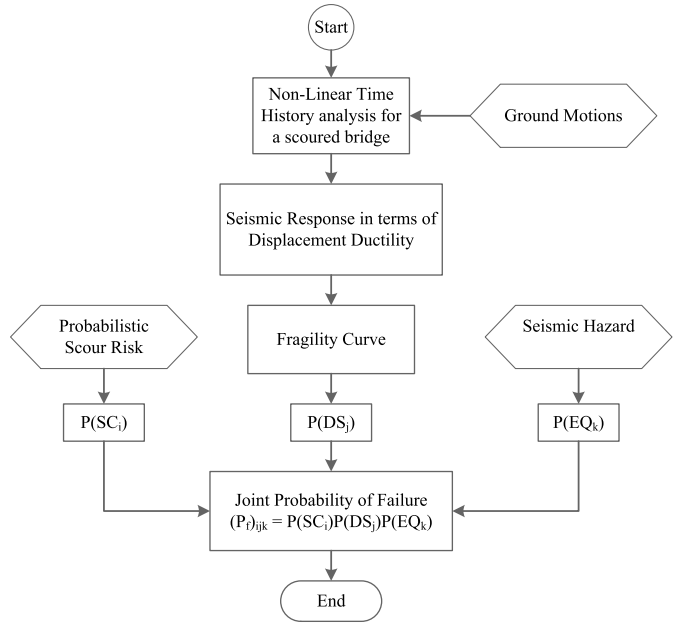

Fig. 1. Flowchart for developing the joint probability of failure for a bridge

$$d_s = K_{yb} K_s K_\theta K_I K_t K_d \tag{1}$$

where K_{yb} = water depth–bridge shape impact factor, as expressed in Eq. (2); K_s = pier-shape correction factor; K_θ = correction coefficient of the angle of attack of flow; K_I = flow intensity correction coefficient; K_t = time-factor correction coefficient; and K_d = river-bed-material characteristic correction coefficient

$$\begin{cases} K_{yb} = 2.4 b_e & \dfrac{b_e}{y} < 0.7 \\ K_{yb} = 2\sqrt{y b_e} & 0.7 < \dfrac{b_e}{y} < 5 \\ K_{yb} = 4.5 y & \dfrac{b_e}{y} > 5 \end{cases} \tag{2}$$

where b_e represents the equivalent pier width perpendicular to the flow; and y = flow depth. In the approach proposed by Melville and Coleman, the equivalent pier width (b_e) plays a key role. Additionally, when the water depth, river-bed location, and pier type are considered, b_e may be slightly different, which can be classified primarily into four cases and are expressed as Eq. (3)

$$\begin{cases} b_e = b_c & Y > b_{pc}\ (\text{Case1}) \\ b_e = b\left(\dfrac{y+Y}{y+b_{pc}}\right) + b_{pc}\left(\dfrac{b_{pc}-Y}{y+b_{pc}}\right) & b_{pc} \geq Y \geq 0\ (\text{Case2}) \\ b_e = b\left(\dfrac{y+Y}{y+b_{pc}}\right) + b_{pc}\left(\dfrac{b_{pc}-Y}{y+b_{pc}}\right) & 0 \geq Y \geq -y\ (\text{Case3}) \\ b_e = b_{pc} & -Y > y\ (\text{Case4}) \end{cases} \tag{3}$$

Eq. (3) shows that b_e is interpolated using b_c and b_{pc}, as shown in Eq. (4)

Downloaded from ascelibrary.org by NTU on 07/11/18. Copyright ASCE. For personal use only; all rights reserved.

$$b_e = \begin{cases} Ab_c + Bb_{pc}, \quad \text{where} \\ A = \dfrac{x_1 y + x_2 Y}{x_3 y + x_4 b_{pc}} \\ B = \dfrac{x_5 b_{pc} - x_6 Y}{x_7 y + x_8 b_{pc}} \\ A + B = 1 \end{cases} \tag{4}$$

where A and B are the weights for b_c and b_{pc}, respectively, and the sum of the two weights is one. According to Melville and Coleman (2000), A and B are functions of the flow depth (y); level of the top surface of the pile cap below the surrounding bed level (Y); and pile-cap width perpendicular to the flow (b_{pc}). In this study, an optimization technique is employed to obtain the functions of A and B, as described in Eq. (4), where x_i refers to the coefficient to be determined. The mathematical formulation of the optimization problem is described as follows:

$$\text{Min}_x D_s - d_s = D_s - f(x) \tag{5}$$

where D_s = scour depth obtained from the experiment; and d_s = calculated scour depth using Eq. (1), which is a function of x described in Eq. (4). The experimental data of the 176 entries are obtained, and the sequential quadratic programming tool from the *MATLAB* toolbox is used to solve the optimization problem described in Eq. (5). The objective of the optimization is to obtain eight coefficients in Eq. (4) that can help minimize the estimation errors. However, when $Y > 2.4b_c$, it is typically not scoured to the location of the pile cap and so that the influence of pile cap and pile groups can be ignored. Therefore, under such conditions, optimization is not performed, indicating that $b_e = b_c$. The optimization results for the other three cases are described in Eqs. (6)–(8)

$$\begin{aligned} b_e &= g(y, Y, b_c, b_{pc}) \\ &= \left(\frac{0.80y + 0.31Y}{0.83y + 1.00b_{pc}}\right) b_c + \left(\frac{0.02b_{pc} - 0.07Y}{0.75y + 0.56b_{pc}}\right) b_{pc} \text{ (Case2)} \end{aligned} \tag{6}$$

$$\begin{aligned} b_e &= h(y, Y, b_c, b_{pc}) \\ &= \left(\frac{0.22y + 0.38Y}{0.16y + 0.31b_{pc}}\right) b_c + \left(\frac{0.05b_{pc} - 0.16Y}{-0.03y + 0.57b_{pc}}\right) b_{pc} \text{ (Case3)} \end{aligned} \tag{7}$$

$$\begin{aligned} b_e &= k(y, Y, b_c, b_{pc}) \\ &= \left(\frac{0.42y + 0.11Y}{0.24y + 0.90b_{pc}}\right) b_c + \left(\frac{0.11b_{pc} - 0.08Y}{0.20y + 1.00b_{pc}}\right) b_{pc} \text{ (Case4)} \end{aligned} \tag{8}$$

Table 1 presents the predicted result of the proposed approach. In general, the result shows that the accuracy of the formula proposed by Melville and Coleman (2000) is significantly improved. The proposed formula is conceptually consistent with the observed scour behaviors and helps predict the scour-depth accurately.

Based on the built scour prediction formula, it is known that scour depth is a function of water depth and water velocity. That is, scour depth is a function of random variables and its probabilistic characteristics (such as mean value, standard deviation, and probability density function) are described using MCS followed by a goodness-of-fit test. The design/target values specified in the code (Ministry of Transportation and Communications 2009) are used as the mean values of water depth and water velocity. Based on earlier studies (Liao et al. 2015), the water depth and water velocity were found to often follow a log-normal distribution and are adopted in this study. In addition, the coefficients of variation for the water depth and water velocity are assumed as 0.135 and 0.35, respectively (Liao et al. 2015).

Table 1. Accuracies Comparison among Different Approaches

Soil covering depth	Mean absolute percentage error (MAPE)	
	Proposed approach	Melville and Coleman (2000)
$Y > 2.4b_c$	5.1	12.22
$2.4b_c > Y \geq 0$	30.4	106.28
$0 > Y > -y$	34.2	93.50
$Y \leq -y$	24.8	236.69
Average	28.9	102.75

Simulation of Nonlinear Behaviors of Pier and Caisson

Two types of mechanical properties of the concrete are considered: the cover and core concretes. The behavior of the cover concrete is considered unconfined using a model proposed by Coronelli and Gambarova (2004). The stress-strain correlation is calculated using Eqs. (9) and (10) for ascending and descending branches, respectively. The parameter ζ represents the softening effect resulting from the corrosion. Because the corrosion is not considered, the value of ζ becomes 1

$$\sigma_a = \zeta f_c \left[2\left(\frac{\varepsilon}{\zeta\varepsilon_0}\right) - \left(\frac{\varepsilon}{\zeta\varepsilon_0}\right)^2\right] \tag{9}$$

$$\sigma_d = \zeta f_c \left[1 - \left(\frac{\frac{\varepsilon}{\zeta\varepsilon_0} - 1}{\frac{2}{\zeta} - 1}\right)^2\right] \tag{10}$$

The strength of the core concrete is greater than that of the cover section because of the presence of transverse reinforcement. The model proposed by Mander et al. (1988) is adopted in this study to evaluate the confinement effect. Because the pier has a solid circular section whereas the caisson has a hollow section, two types of core concretes are considered. The circular section is evaluated using the model proposed by Mander et al. (1988). However, the hollow section should be modified to consider the different force distributions. The general equation of the model proposed by Mander is expressed in Eq. (11)

$$f_c = \frac{f'_{cc} x r}{r - 1 + x^r} \tag{11}$$

where f_c = longitudinal compressive concrete stress; and f'_{cc} = compressive strength for the confined concrete, which can be determined as follows:

$$f'_{cc} = f'_{co}\left(-1.254 + 2.254\sqrt{1 + \frac{7.94 f'_l}{f'_{co}}} - 2\frac{f'_l}{f'_{co}}\right) \tag{12}$$

where f'_{co} = unconfined concrete compressive strength; and f'_l = effective confining stress on the concrete. The variable x in Eq. (11) is calculated as follows:

$$x = \frac{\varepsilon_c}{\varepsilon_{cc}} \tag{13}$$

where ε_c = longitudinal compressive concrete strain; and ε_{cc} is calculated as follows:

Downloaded from ascelibrary.org by NTU on 07/11/18. Copyright ASCE. For personal use only; all rights reserved.

$$\varepsilon_{cc} = \varepsilon_{co}\left[1 + 5\left(\frac{f'_{cc}}{f'_{co}} - 1\right)\right] \tag{14}$$

where ε_{co} is the corresponding unconfined concrete strain of f'_{co} and is 0.002, as suggested by Mander et al. (1988). The variable r in Eq. (11) is calculated as follows:

$$r = \frac{E_c}{E_c - E_{\text{sec}}} \tag{15}$$

where $E_c = 5{,}000\sqrt{f'_{co}}$ MPa is the tangent modulus of elasticity of the concrete and

$$E_{\text{sec}} = \frac{f'_{cc}}{\varepsilon_{cc}} \tag{16}$$

For foundation with a hollow section (i.e., the investigated bridge), the effective confined stress (f'_l) is different from that of a solid pier and is determined using Eq. (17)

$$f'_l = \text{effective confinement pressure} = k_e f_l = k_e\left[\frac{2f_{yh}A_{sp}}{s(d_{s_2} - d_{s_2})}\right] \tag{17}$$

The stress–strain curve of the steel used in this study is described as follows:

For $0 \le \varepsilon_s \le \varepsilon_y$

$$f_s = E_s\varepsilon_s \tag{18}$$

For $\varepsilon_y \le \varepsilon_s \le \varepsilon_{sh}$

$$f_s = f_y \tag{19}$$

For $\varepsilon_{sh} \le \varepsilon_s \le \varepsilon_{su}$

$$f_s = f_y\left[\frac{f_u}{f_y} - \left(\frac{f_u - f_y}{f_y}\right)\left(\frac{\varepsilon_u - \varepsilon_s}{\varepsilon_u - \varepsilon_{sh}}\right)^2\right] \tag{20}$$

where f_s = stress of the steel; E_s = elastic modulus of the steel; ε_s = strain in the steel; f_y = yield stress of the steel; f_u = ultimate stress of the steel; ε_{sh} = strain hardening of the steel; and ε_u = ultimate steel strain.

According to Sung et al. (2005), the shear mode should be converted to the corresponding bending mode to determine the failure mode of the pier or caisson. Accordingly, three types of failure modes are classified: shear failure mode, flexural-to-shear failure mode, and flexural failure mode. The nonlinear behaviors of the pier and caisson are largely described via the P-M3 plastic hinge using the proposed *SAP2000* model. The shear plastic hinge is not used.

Simulation of Nonlinear Behaviors of Soil

Many methods are available to model the soil behavior. The regulations suggested by the Taiwan code are adopted in this study (Chang et al. 2009). The soil behavior is simulated using the bilinear link element provided in *SAP2000*. The link is divided into three types, which include horizontal resistance on the peripheral side of the caisson, and vertical and friction resistances on the bottom plane of the caisson. The soil behavior is simulated using a bilinear model where the passive earth force is employed as the upper bound. The friction effect between the caisson and the soil along the peripheral side area is ignored. Similarly, the link property in the vertical direction of the bottom surface is simulated using a bilinear model where the bearing force is employed to determine the upper limit, as shown in Eq. (21). The stiffness in the linear part is simulated using Eq. (22). The upper limit and stiffness in the linear part for the frictional force are described in Eqs. (23) and (24), respectively. The friction link is placed at the bottom of the caisson using the same partition method

$$q_u = \alpha c N_c + \gamma_2 D_f N_f + 0.5\beta\gamma_1 B N_r \tag{21}$$

where q_u = bearing force; α and β = base factors based on the foundation shape; c = soil cohesion; γ_1 = effective unit of the bottom surface of the lower base of the soil; γ_2 = average effective unit weight of the soil above the bottom surface; D_f = foundation depth; B = base width of the foundation; and N_c, N_f, and N_r = factors for the supporting forces

$$k_v = k_{v0}(B_v/30)^{-3/4} \tag{22}$$

where k_{vo} = coefficient of the vertical ground reaction force; and B_V = base equivalent load width

$$R_f = N\tan\delta + AC_a \tag{23}$$

$$k_s = 0.3k_v \tag{24}$$

where R_f = frictional resistance of the bottom surface (tf) (1 tf = 9806 N); N = effective vertical load acting on the basis (tf); δ = angle of friction (degrees); A = effective contact area between the bottom surfaces of the base (m^2); and C_a = effective adhesion (t/m^2).

Ground Motions and Seismic Hazard

A series of nonlinear time-history analyses are performed to develop the fragility curve. Based on the AASHTO guide specification for load and resistance factor design (LRFD) seismic bridge design (AASHTO 2012), a nonlinear time-history analysis should be performed for critical and essential bridges as approved, for which the definitions, limitations, and requirements are given in Section 1.3.5 of the AASHTO guide specification for LRFD seismic bridge design (AASHTO 2012). The design action is considered to be the maximum response calculated for three ground motions in each principal direction. If a minimum of seven time histories are used for each component of motion, the design actions are considered as the mean responses calculated for each principal direction. According to the AASHTO guide specification for LRFD seismic bridge design (AASHTO 2012), seven ground motions obtained from the PEER ground motion are used in the nonlinear time history in this study. As indicated in AASHTO (2012), "response-spectrum-compatible time histories are used developed from the representative recorded motion (p. 4-86–4-87)." Specifically, a response-spectrum-compatible time history refers to the response spectrum of the selected earthquakes falling in between 0.2 and 1.5 T (where T is the fundamental period); however, it may not be less than 90% of the corresponding design spectral acceleration for a damping ratio of 5%. In addition, the average value of the response spectrum within the designated period range may not be less than the average value of the corresponding design spectral accelerations. The ground motions used in this study are converted into response-spectrum-compatible data for return periods of 30, 475, and 2,500 years.

This study aims to investigate the safety of the bridge against two hazards simultaneously through a probabilistic approach. The probability density distributions of the scour and earthquake magnitudes are incorporated into the evaluation process. The aforementioned probabilistic scour curve is used to address this fact with respect to the flood hazard. The seismic risk is measured using

Downloaded from ascelibrary.org by NTU on 07/11/18. Copyright ASCE. For personal use only; all rights reserved.

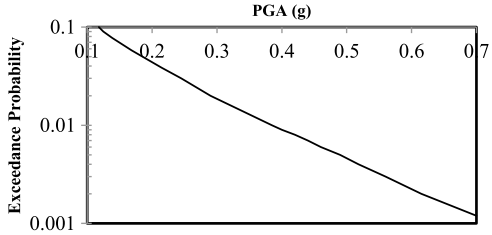

Fig. 2. Seismic hazard curve for investigated bridge (adapted from Yeh and Jean 2007)

PSHA. The purpose of PSHA is to evaluate the hazard of seismic ground motion at a site by considering all possible earthquakes in the area, estimating the associated shaking at the site, and calculating the probabilities of these occurrences (McGuire 2004). There are many assessments for seismic hazard analysis and two recent works related to Taiwan are described subsequently. Campbell et al. (2002) developed a seismic hazard model for Taiwan to estimate earthquake losses and risk management. Their seismic hazard model is composed of two major components: a seismotectonic model, and a ground-shaking model. Seismic hazard curves at a grid of sites across the island of Taiwan were calculated resulting in to a seismic hazard map. Wang et al. (2015) developed a seismic hazard assessment using MCS with earthquake statistics and local ground motion models. They found that the current seismic design in Taipei might not be as conservative as expected. Although the seismic hazard is important, developing a new seismic hazard model is beyond the scope of the current study. Instead, the model built from NCREE is commonly accepted in Taiwan, and therefore is adopted in this paper. For details please refer to Yeh and Jean (2007). Based on their model, a seismic hazard curve at a location close to the investigated bridge is built, as shown in Fig. 2.

Construction of Fragility Curve

The displacement ductility (μ_Δ) is used to measure the structural performance under seismic excitations. The displacement ductility is defined as the ratio of the displacement of the bridge girder to the yield displacement of a pier, as indicated in Eq. (25) (Caltrans 2006)

$$\mu_\Delta = \mu_D/\mu_y \tag{25}$$

The yield displacement for a pier is the product of the yield rotation of the plastic section and the length of the pier, as shown in Eq. (26)

$$\mu_y = \theta_y l \tag{26}$$

where θ_y is the yield rotation corresponding to the condition where the reinforced bar starts to yield in the plastic hinge.

Eq. (27) is used to establish the relationship between the PGA and the displacement ductility

$$\mu_\Delta = a(PGA)^b \tag{27}$$

In this case, a and b are constants derived from the regression analysis. The fragility curve is a conditional probability computation, representing a failure probability for a given intensity measurement. For example, when the PGA is given, assuming that the capacity and demand of the bridge are log-normally distributed, the corresponding failure probability can be calculated using Eq. (28) as follows:

$$P_f(\mu_\Delta > \mu|\mathrm{PGA} = x) = 1 - \Phi\left(\frac{\ln\left(\frac{\mu}{a\mathrm{PGA}^b}\right)}{\sigma_{\mu_\Delta|\mathrm{PGA}}}\right) \tag{28}$$

where μ = mean value of the capacity (Alipour et al. 2013); $a \times \mathrm{PGA}^b$ = mean value of the demand in terms of the displacement ductility; σ = standard deviation with respect to the limit state; and Φ = cumulative probability density function of the standard normal. Based on the study by Alipour et al. (2013), the capacity of the displacement ductility for varied limit states are $1 < \mu < 2$, $2 < \mu < 4$, $4 < \mu < 7$, and $\mu > 7$ for slight, moderate, major, and complete collapse damages, respectively. The standard deviation for a given PGA ($\sigma_{\mu_\Delta|\mathrm{PGA}}$) is calculated using Eq. (29)

$$\sigma_{\mu_\Delta|\mathrm{PGA}} = \sqrt{\sigma^2_{D|\mathrm{PGA}} + \sigma^2_c} \tag{29}$$

where $\sigma_{D|\mathrm{PGA}}$ = standard deviation of the demand for a given PGA; and σ_c = standard deviation of the capacity (i.e., 0.5) (Chang et al. 2009). The is obtained by performing another regression analysis, as indicated in Eq. (30)

$$\sigma_{D|\mathrm{PGA}} = c(\mathrm{PGA})^f \tag{30}$$

Case Study

General Information of the Investigated Bridge

The Nanyun Bridge, located in the central Taiwan, is selected for the case study. Specifically, Pier 14 (P14), Pier 15 (P15), and the superstructure between them are considered. Both piers are solid concrete section. However, the caissons below are hollow cylinders with an outside diameter of 5.5 m and an inside diameter of 4.5 m. The concrete strengths are 28 and 21 MPa for the bridge pier and caisson, respectively. The SD280 steel bar is used for diameters less than or equal to 16 mm while SD420W is used for diameters greater than 16 mm.

Analyses Results

The MCS is used to simulate the variation in the scour depth for the Nanyun Bridge, where the water depth and water velocity are reproduced via LN (1.5933, 0.1798) and LN (0.6692, 0.4173), respectively (Liao et al. 2015). The histogram of scour depth is obtained through a simulation with a sample size of 10^6. Based on the histogram, the scour risk curve can be established, as shown in Fig. 3.

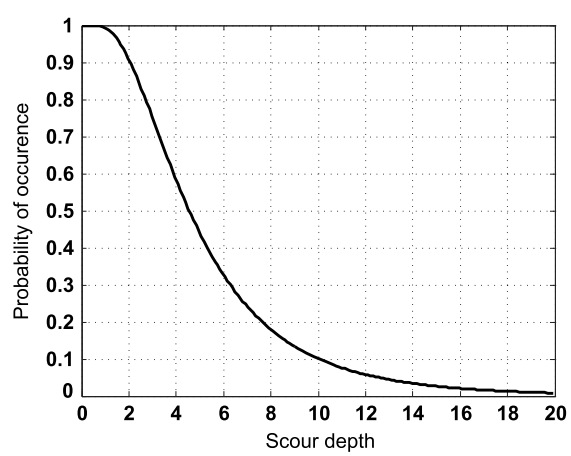

Fig. 3. Risk curve of scour depth at Nanyun Bridge

J. Perform. Constr. Facil., 2018, 32(3): 04018017

Downloaded from ascelibrary.org by NTU on 07/11/18. Copyright ASCE. For personal use only; all rights reserved.

Table 2. Summary of Total Time-History Analyses Conducted in This Study

Name	Earthquake	PGA (return period)	Scour depth	Total number
Contents	San Fernando			105
	Imperial Valley	0.091 (30 years)		
	Loma Prieta	0.363 (475 years)	4	
	Northridge	0.453 (2,500 years)	8	
	Kobe	1.007	10	
	Chi-Chi (TCU52)	1.510		
	Chi-Chi (TCU68)			

Table 3. PGAs Corresponding to μ_Δ and $\sigma_{D|PGA}$ for Scour Depth of 4 m

PGA	Mean of μ_Δ	$\sigma_{D\|\mathrm{PGA}}$
0.091	0.318	0.012
0.363	1.243	0.095
0.453	1.600	0.133
1.007	4.756	0.545
1.510	5.118	0.802

Table 4. PGAs Corresponding to μ_Δ and $\sigma_{D|\mathrm{PGA}}$ for Scour Depth of 8 m

PGA	Mean of μ_Δ	$\sigma_{D\|\mathrm{PGA}}$
0.091	0.386	0.0217
0.363	1.402	0.0826
0.453	1.635	0.118
1.007	5.634	1.080
1.510	6.312	1.069

Table 5. PGAs Corresponding μ_Δ and $\sigma_{D|\mathrm{PGA}}$ for Scour Depth of 10 m

PGA	Mean of μ_Δ	$\sigma_{D\|\mathrm{PGA}}$
0.091	0.493	0.035
0.363	1.934	0.146
0.453	2.353	0.240
1.007	5.616	0.889
1.510	8.485	0.934

To determine the failure probability of the scoured Nanyun Bridge for a given PGA, three different scour depths and five different sets of ground motions are used. A total of 105 time-history analyses are performed, as given in Table 2. In addition to return periods of 30, 475, and 2,500 years, this study performs another two sets of ground motions corresponding to PGAs of 1.007 and 1.510. To draw a fragility curve for a given limit state, a continuous failure-probability function in terms of PGA is required. The 105 time-history analyses only provide failure probabilities at five different PGA values. Therefore, as explained, the regression analysis is employed to build the fragility curve. Table 3 lists the mean values and standard deviations of the ductility displacement for a bridge with a scour depth of 4 m under five different PGA values. Each set of PGA has seven different ground motions. The average of the seven responses yields the mean value. Similarly, Tables 4 and 5 list mean values and standard deviations of the ductility displacement for a bridge with scour depths of 8 and 10 m under five different PGA values, respectively. Table 6 provides detailed regression results for mean and standard deviation of displacement ductility for scour depths of 4, 8, and 10 m.

Table 6. Regression Results for Mean and Standard Deviation of Displacement Ductility for Scour Depths of 4, 8, and 10 m

Scour depth (m)	Constant			
	a	b	c	f
4	3.80	1.04	0.46	1.53
8	4.40	1.05	0.60	1.51
10	5.48	1.01	0.65	1.25

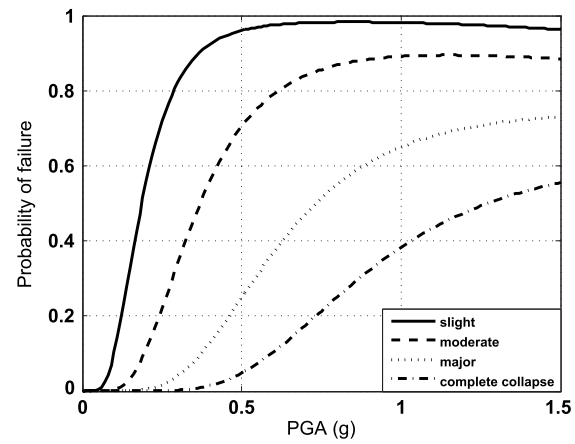

Fig. 4. Fragility curves for a bridge with scour depth of 10 m

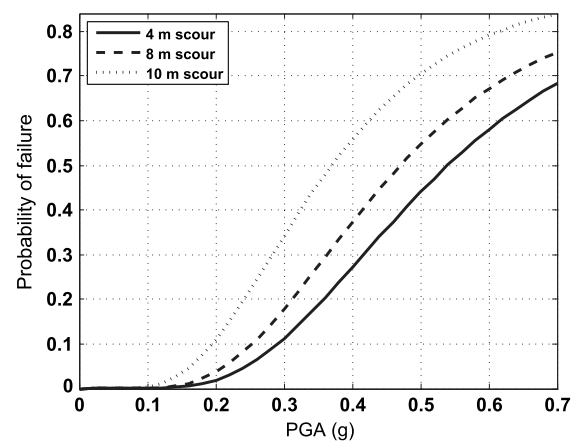

Fig. 5. Fragility curves with different scour depths under moderate-damage state

Fig. 4 shows the fragility curves for a bridge with scour depths of 10 m. Fig. 5 shows the fragility curves with different scour depths at moderate damage state. The results show that the failure probability increases with the increase in the scour depth and decreases as the limit state changes from slight to collapse. More importantly, the failure probability was found to increase significantly as the scour depth changes from 8 to 10 m for each limit state.

The probability of bridge failure by exceeding a given limit state of k, DS_k, under the scour event of SC_i, and the earthquake demand of EQ_j can be calculated as shown in Eq. (31) (Alipour et al. 2013)

$$(P_f)_{ijk} = P(SC_i \cap DS_j \cap EQ_k) \tag{31}$$

The probability of the simultaneous occurrence of two extreme events (i.e., scour and earthquake) is generally small. Three models

Downloaded from ascelibrary.org by NTU on 07/11/18. Copyright ASCE. For personal use only; all rights reserved.

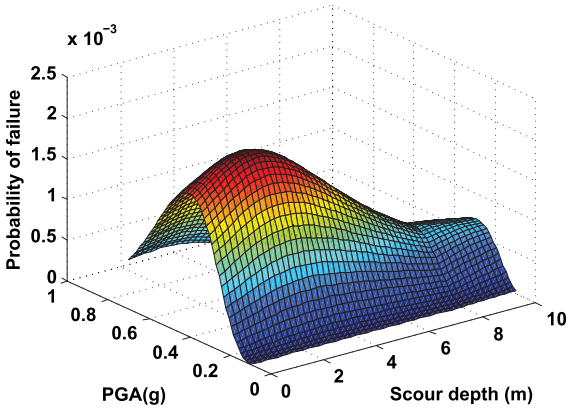

Fig. 6. Joint probability of failure for moderate-damage state at Nanyun Bridge

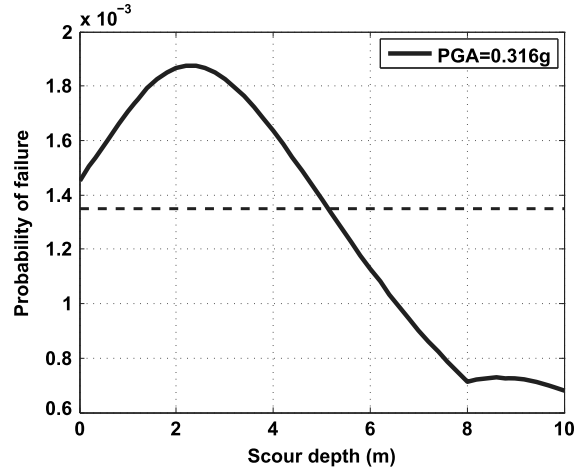

Fig. 7. Joint failure probability of Nanyun Bridge for moderate-damage state at design PGA

for considering the combination effects of extreme loads using reliability approaches are often adopted in practical applications. They are: (1) Turkstra's rule, (2) the Ferry Borges–Castanheta model, and (3) Wen's load coincidence method (Ghosn et al. 2003). Turkstra's model considers one load reaching its maximum value combined with another load with its mean value, which looks rational, but the results are generally unconservative (Sun et al. 2014). Conversely, the Ferry Borges model is more accurate than Turkstra's rule because it takes the rate of occurrence of the loads and their time duration into consideration (Ghosn et al. 2003). The Turkstra's rule and the Ferry Borges–Castanheta model assume independence between two different load types. Conversely, Wen's method considers the rate of occurrence of each load event and the rate of simultaneous occurrences of a combination of two or more correlated loads (Wen 1990). Many researchers have made great efforts on investigating the load combination effect. It is very unusual to find scour occurs that follow earthquakes in Taiwan. This study investigated the safety performance of a scoured bridge under seismic excitations. The time difference between the occurrence of a flood and an earthquake would justify assuming independence between earthquakes and scour events. Thus, this study considers the occurrence probabilities of scour and earthquake events to be statistically independent in calculating their combination effects using simulation approach. Eq. (31) can be calculated as shown in Eq. (32)

$$(P_f)_{ijk} = P(SC_i)P(DS_j)P(EQ_k) \tag{32}$$

In this case, $P(SC_i)$ is the probability of experiencing the ith scour scenario, which is obtained from the scour risk curve, shown in Fig. 3; $P(DS_j)$ is the probability of failure under a specific-damage state, which is estimated from the seismic-fragility curve obtained for different scour depths as shown in Figs. 4 and 5; and $P(EQ_k)$ is the occurrence probability of the kth earthquake scenario defined in the probabilistic seismic-hazard curve in terms of PGA as shown in Fig. 2. The joint-failure probabilities are developed within a PGA range of 0.1–0.7 because of the data span of the NCREE seismic-hazard curve. Interpolation and extrapolation are used to estimate the failure probability for scour depths of 4, 8, and 10 m. Fig. 6 shows the joint probability of failure for moderate damage state.

A deterministic design value (i.e., scour depth), considering both the hazards, for a given reliability target is derived to help engineers in their present design processes as described subsequently. The three-dimensional (3D) plot of the joint probability of failure (Fig. 6) is reduced to a two-dimensional (2D) plot using a fixed PGA value. To be compatible with the present practice, the design PGA of the Nanyun Bridge is used (i.e., 0.32 g). Fig. 7 illustrates an example for the moderate damage state. If the target of reliability index (β) is 3, the required scour depth can be derived, which is approximately equal to 5 m as indicated in Fig. 7. That is, engineers can follow their regular process in designing bridges, and if the safety of a bridge with a scour depth of 5 m is confirmed the reliability of such bridges against floods and earthquakes is ensured at a value of 0.99865 for a moderate damage state.

A sudden increase in the probability is observed for scour depths greater than 8 m, as shown in Figs. 6 and 7. The joint-failure probability increases if the scour depth is greater than 8 m. As shown in Eq. (32), the joint-failure probability largely depends on two probabilities: the probability of a given scour depth $[P(SC_i)]$ and failure probability of a bridge with the specified scour depth $[P(DS_j)]$. The occurrence rate of a given scour depth $[P(SC_i)]$ is a monotonically decreasing function, as shown in Fig. 3. However, the failure probability of the Nanyun Bridge increases significantly for scour depths greater than 8 m, as shown in Fig. 5. The caisson depth for the Nanyun Bridge is approximately 14 m, thereby increasing the failure probability considerably. The failure probability dominates the joint probability for all the damage states in this case study.

Conclusions

Bridges are important infrastructures and their safety should be ensured. Based on the literature, both floods and earthquakes are found to be the primary threats concerning the safety of bridges in Taiwan. The uncertainties involved in such hazards are inevitable, hence a probabilistic approach is employed in this study. This study integrates the nonuniform scour-depth prediction, nonlinear time-history analyses, nonlinear soil property, and moment-curvature analyses to establish fragility curves to evaluate the safety of a bridge against floods and earthquakes. To demonstrate the proposed evaluation process, the Nanyun Bridge, which is located in the Nantou County, is selected for the case study. Piers 14 and 15 of the Nanyun Bridge are modeled for a sour depth of 4 m, which is currently observed. The plastic hinges are predefined at each pier located 1 m below the ground level because of the presence of nonlinear soil link. Based on the results, the conclusions of this study are as follows:

- The Nanyun Bridge is likely to experience a flood scour with a depth in the range of 3–5 m, based on calculations from

Downloaded from ascelibrary.org by NTU on 07/11/18. Copyright ASCE. For personal use only; all rights reserved.

the proposed formula, which is consistent with the on-site observation;

- The failure probability for each limit state is insignificant. The failure probability is significant only for the slight and moderate damage states. For example, the failure probabilities are 0.42 and 0.84 for moderate and slight limit states, respectively (for a PGA of 0.5 g and a scour depth of 4 m);
- The failure probability against seismic attacks is not proportional to the scour depth. The results show that the failure probability does not significantly increase when the scour depth increases from 4 to 8 m. However, the failure probability considerably changes when the scour depth increases from 8 to 10 m. This significant change in the failure probability affects the shape of the joint-failure probability in the range of 8–10 m; and
- A deterministic design value, considering both the scour and seismic hazards, is proposed for a given reliability target. For example, if the reliability target index (β) of 3 is specified, the corresponding design scour depth is approximately 5 m for the moderate limit state.

Acknowledgments

This study was supported by the TU-NTUST Joint Research Program. The support is gratefully acknowledged.

References

AASHTO. (2012). "AASHTO LRFD bridge design specifications." Washington, DC.

Alipour, A., Shafei, B., and Shinozuka, M. (2013). "Reliability-based calibration of load and resistance factors for design of RC bridges under multiple extreme events: Scour and earthquake." *J. Bridge Eng.*, 10.1061/(ASCE)BE.1943-5592.0000369, 362–371.

Andrić, J. M., and Lu, D. G. (2016). "Risk assessment of bridges under multiple hazards in operation period." *Saf. Sci.*, 83, 80–92.

Basoz, N. I., Kiremidjian, A. S., King, S. A., and Law, K. H. (1999). "Statistical analysis of bridge damage data from the 1994 Northridge, CA, earthquake." *Earthquake Spectra*, 15(1), 25–54.

Caltrans. (2010). "Seismic design criteria version 1.6." Sacramento, CA.

Campbell, K. W., Thenhaus, P. C., Barnhard, T. P., and Hampson, D. B. (2002). "Seismic hazard model for loss estimation and risk management in Taiwan." *Soil Dyn. Earthquake Eng.*, 22(9), 743–754.

Chang, K. C., et al. (2009). "Seismic assessment and retrofit manual for highway bridges." *NCREE 0-09-028*, National Center for Research on Earthquake Engineering, Taipei, Taiwan.

Coronelli, D., and Gambarova, P. (2004). "Structural assessment of corroded reinforced concrete beams: Modeling guidelines." *J. Struct. Eng.*, 10.1061/(ASCE)0733-9445(2004)130:8(1214), 1214–1224.

Davis-McDaniel, C., Chowdhury, M., Pang, W. C., and Dey, K. (2013). "Fault-tree model for risk assessment of bridge failure: Case study for segmental box girder bridges." *J. Infrastruct. Syst.*, 10.1061/(ASCE)IS.1943-555X.0000129, 326–334.

Elnashai, A. S., et al. (2012). "The Maule (Chile) earthquake of February 27, 2010: Development of hazard, site specific ground motions and back-analysis of structures." *Soil Dyn. Earthquake Eng.*, 42, 229–245.

Ghosn, M., Moses, F., and Wang, J. (2003). *Design of highway bridges for extreme events*, Vol. 489, National Cooperative Highway Research Program, Washington, DC.

HEC-18 (Hydraulic Engineering Circular-18). (2012). *Evaluating scour at bridges*, 5th Ed., U.S. Dept. of Transportation, Springfield, VA.

Honjo, Y., Kusakabe, O., Matsui, K., Kouda, M., and Pokhard, G. (2002). "Foundation design codes and soil investigation in view of international harmonization and performance based design." *Proc., IWS Kamakura Conf*, A.A. Balkema, Amsterdam, Netherlands.

Hsu, Y. T., and Fu, C. C. (2004). "Seismic effect on highway bridges in Chi Chi earthquake." *J. Perform. Constr. Facil.*, 10.1061/(ASCE)0887-3828(2004)18:1(47), 47–53.

Liao, K. W., Lu, H. J., and Wang, C. Y. (2015). "A probabilistic evaluation of pier-scour potential in the Gaoping river basin of Taiwan." *J. Civ. Eng. Manage.*, 21(5), 637–653.

Mander, J. B., Priestley, M. J., and Park, R. (1988). "Theoretical stress-strain model for confined concrete." *J. Struct. Eng.*, 10.1061/(ASCE)0733-9445(1988)114:8(1804), 1804–1826.

MATLAB [Computer software]. MathWorks, Natick, MA.

McGuire, R. K. (2004). *Seismic hazard and risk analysis*, Earthquake Engineering Research Institute, Oakland, CA.

Melville, B. W., and Coleman, S. E. (2000). *Bridge scour*, Water Resources Publications, LLC.

Ministry of Transportation and Communications. (2009). "Code for design of highway bridges." Taipei, Taiwan.

Padgett, J., et al. (2008). "Bridge damage and repair costs from Hurricane Katrina." *J. Bridge Eng.*, 10.1061/(ASCE)1084-0702(2008)13:1(6), 6–14.

SAP2000 [Computer software]. Computers and Structures, Inc., Walnut Creek, CA.

Sun, D., Wang, X., and Sun, B. (2014). "A methodology for multihazards load combinations of earthquake and heavy trucks for bridges." *Sci. World J.*, 2014, 1–9.

Sung, Y. C., Liu, K. Y., Su, C. K., Tsai, I. C., and Chang, K. C. (2005). "A study on pushover analyses of reinforced concrete columns." *J. Struct. Eng. Mech.*, 21(1), 35–52.

Wang, J. P., Wu, Y. M., and Huang, D. (2015). "Major earthquakes around Taipei and a seismic hazard assessment with Monte Carlo simulation." *Nat. Hazard. Rev.*, 10.1061/(ASCE)NH.1527-6996.0000176, 04015003.

Wen, Y. K. (1990). *Structural load modeling and combination for performance and safety evaluation*, Elsevier Science, Atlanta.

Yeh, C. H., and Jean, W. Y. (2007). "Study on the integration of seismic hazard analysis and disaster simulation technology (II)." *NCREE-07-040*, National Center for Research on Earthquake Engineering, Taipei, Taiwan.

Downloaded from ascelibrary.org by NTU on 07/11/18. Copyright ASCE. For personal use only; all rights reserved.